IJCRT.ORG ISSN : 2320-2882

INTERNATIONAL JOURNAL OF CREATIVE RESEARCH THOUGHTS (IJCRT)

An International Open Access, Peer-reviewed, Refereed Journal

Photochemistry Of Volatile Uranium Compounds

Anamika[1] and Anjani Kumar Shukla[2]

[1]Head, University Department of Chemistry, Jamshedpur Women's University, Jamshedpur (Jharkhand)

[2]Department of Chemistry, Assistant Professor (Guest Teacher) R.D.S.College, Muzaffarpur (Bihar)

Abstract: Examinations of the photochemical literature of uranium compounds clearly indicate that attention has been given to uranium hexafluoride (UF_6) extensively. The economics of laser isotope separation have dictated the directions of much of the applied photochemical research on UF_6 and other volatile uranium compounds. Presently, we report the photochemical investigations carried out in our laboratory on various volatile uranium compounds namely UF_6, uranium tetrahydroborate, $U(BH_4)_4$ and uranyl hexafluoro-acetylacetonate tetrahydrofuran $UO_2(hfacac)_2$. THF using conventional lamps and various lasers sources in UV/visible and infracted regions. Incidentally we have demonstrated laser isotope separation of uranium using the last compound.

Key words: Uranium hexafluoride, Laser isotope separation, Conventional lamps, UV-visible.

INTRODUCTION

The demand for enriched uranium as a fuel source in nuclear fission reactors has directed a large amount of research in recent years towards the development of more efficient and economic isotope separation method. The ideas of selective photochemistry as a means of uranium isotope separation dates back to the Manhattan Project. This work met with little success and was abandoned as various other methods like mass diffusion, centrifugation etc. bean to yield positive results. But the advent of lasers has stimulated reconsideration of the photochemical process.

Choice of an appropriate molecular form of uranium is an important first step in developing such a process. Almost all work has been devoted to gas phase chemical processes rather than solid or liquid due principally to the tendency for isotope effects to be obscured by collective interactions within the condensed phase. Hence, it becomes desirable to work with a molecular form which has high vapour pressure to maximize the working density and throughput. Uranium hexafluoride has the highest vapour pressure of any uranium compound and its industrial production and handling has been well developed for existing diffusion and centrifuge methods. It has therefore been automatically a preferred choice for the scheme. The photochemical isotope separation schemes have directed considerable renewed attention to the detailed investigations of gas phase photophysics and photochemistry of UF_6. The economics of isotope separation have consequently dictated the direction of much of the applied photochemical research on UF_6, and other volatile uranium compounds. Presciently, we report the photochemical investigations carried out in our laboratory on the following volatile uranium compounds using conventional lamp and various lasers sources in UV/visible and infrared regions.

1. Uranium hexafluoride UF_6
2. Uranium tetrahydroborate, $U(BH_4)_4$
3. Uranyl hexafluoro-acetylacetonate tetrahydrofuran $UO_2(hfacac)_2$. THF

Uranium hexafluoride, UF_6

The chief advantage of UF_6 for use in LIS schemes is its known spectroscopy, thermal stability and monoisotopy of fluorine. In its 16 μm IR absorption band, the ν_3 mode has a marked isotope shift of 0.65 cm^{-1} at 625cm^{-1}. In the molecular approach schemes of LIS, selective excitation of the desired isotopic species can thus be achieved by a suitable IR laser in 16μm region. In view of this, two approaches appear to be promising for collecting the desired excited isotopic species. The first approach is based on massive multiphotom excitation of UF_6 using one or more IR frequency in its ground electronic state so that the molecule absorbs sufficient energy to unimolecularly dissociate. In the second approach, a limited vibrational selective excitation is followed by an electronic excitation with a suitable UV-visible laser to decompose the excited molecule. The objective of either of these approaches is to maximize selective photodissociation of the desired isotopic species. The parameters which limit the selectivity, in addition to spectroscopic factors, are:-

1. The unimolecular decomposition rates which are in competition with collisional energy exchange losses, and
2. The photodecomposition rates and modes of the electronic excited state.

Therefore, here we present the electronic photochemistry of UF_6 and subsequently its photochemistry in IR region.

ELECTRONIC PHOTOCHEMISTRY

The absorption spectrum of UF_6 in the range 190-410 nm is shown in fig. 1. A strong absorption in the range 200-300 nm is due to electronic transition s from the filled orbitals of the fluorine atoms to the unoccupied orbitals of the uranium atom (charge transfer transitions). Three absorption bands are observed in the vicinity of 214, 260 and 368 nm; the first two bands overlap strongly. In the region of 260 nm (B-X transition) and of 368 nm (A-X transition) there are many weaker bands which can be attributed to electric-dipole forbidden even-even or odd-odd triplet Laports transition.

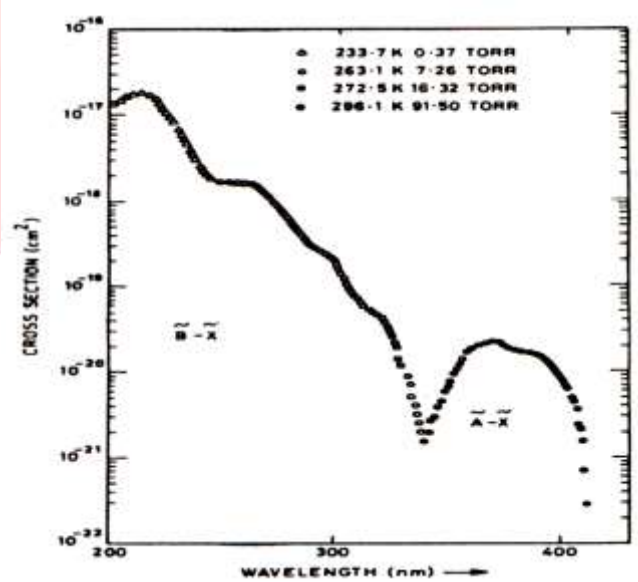

Fig. 1 – Composite electronic absorption spectrum of UF_6 from data taken at various temperatures

The existing literature on UF_6 photolysis is confined to the A-X band, which is also a weakly fluorescent excited state. Much of the reported work monitored the fluorescence to obtain the quenching rate with various additives, including self quenching by UF_6. At low pressures and in the absence of additives the life time of A-X band excitation is about 400 ns at 30°C, rather large to be useful for isotopic enrichment. The lifetime also decrease very rapidly in the presence of additives, especially hydrocarbons, but it is not yet known whether the high quenching rates definitely involve chemical reactions which can be used as a means of collecting the selectively excited species. The only indication about the UF_6 photo decomposition in the

A–X band where quantum yield of about 0.1 was reported. We have investigated the UV photochemistry in its B–X band of UF_6 alone or with hydrogen using 253.7 nm Hg lamps and 337 nm N_2 laser.

UF_6 was purified from HF and other volatile impurities by a dynamic fractional condensation technique where UF_6 condensed in a cold trap at 196 K and the impurities were pumped out. Photolysis at 253.7 nm was conducted in a photochemical reactor. The reactor consisted of a cylindrical array of sixteen low pressure Hg Lamps, providing flux of 1.6 X 10^{16} photons cm^{-3} s^{-1} at sample position in the center. A Molectron UV 400 pulsed N_2 laser was used for irradiations at 337 nm. The pulse width of the laser was 10 ns and at a repetition rate of 10 Hz, its peak energy is 250 mJ/pulse. The all-metal gas handling vacuum system and the cell were leak tested and evacuated to 10^{-6} Torr while baking. The cell was well passivated by prolonged exposure to UF_6 before filling with experimental samples.

In both these cases, the decomposition of UF_6 yielded a mixture of solid products UF_5 and UF_6 the amount of UF_6 formation was more in the mixture than in neat of UF_6. The quantum yield was found to improve with added hydrogen compared to neat system. Although the absorption cross section increases steadily from 4 x 10^{-21} cm^2 and 337 nm to 1.5 x 10^{-18} cm^2 253.7 nm, the quantum yield was found to decrease from 0.14 to about 0.07 towards shorter wavelength. Combining our result with the fact that no fluorescence originated in B–X band indicates the presence of strong non-radioactive process which becomes more prominent at shorter wavelength. The fact that the dissociation product is solid is of tremendous importance. It implies that the separation of enriched products from the feed material is simple as it involves only phase separation. Also isotopic scrambling between enriched product and feed material is likely to be minimum or absent.

Analysis of results of UV photolysis of UF_6 molecules in a mixture with hydrogen and without it permits to look into the main processes. The primary photolysis step is unimolecular dissociation of the UF_6 molecule when the electronic excitation energy exceeds the dissociation threshold:

$UF_6 \rightarrow UF_5$ (gas) + F – 80.77 kcl/mole ……………………………........……… (1)

The subsequent reactions are the combination of the UF_5 monomers into dimmers (kd = 4 x $10^{-11} cm^3 s^{-1}$) and the recombination of the UF_5 monomers with fluorine atoms (kr = 1 x $10^{-11} cm^3 s^{-1}$), whereupon both the dimmers and the regenerated UF_6 are formed in an excited state and may decompose again unless they are collisionally stabilized.

In presence of hydrogen, subsequent exothermic reaction takes place between the newly formed atomic fluorine and hydrogen with k_{fH} = 2.5 x 10^{-11} $cm^3 s^{-1}$ thus preventing reliably the recombination of fluorine with UF_6:

F + $H_2 \rightarrow$ HF + H + 31.1 kcal/mole ....……………………………………… (2)

In presence of hydrogen, the activated UF_6 molecule can also react with molecular hydrogen:

$UF_6 + H_2 \rightarrow (UF_5)$ gas + HF + H – 36.4 kcl/mole ………….........................………..…….. (3)

The photolysis involves also the molecules whose excitation energy is insufficient for dissociation in absence of hydrogen. Both channels are highly endothermic but the second is thermodynamically more favourable. It is most likely that both these processes take place simultaneously at different rates, depending on the experimental conditions and they can be regarded as a single, first stage of the photolysis in presence of hydrogen.

When the reactions in the second stage of the process are examined, the atomic hydrogen formed in the first stage of the process reacts with UF_6 with k_H=1.7x10^{-17} cm^{3}s^{-1}.

$UF_6 + H \rightarrow UF_5 + HF + 67.8$ kcl/mole ..... (4)

The activation energy of bimolecular reaction of UF_6 in the first stage is in excess of 30 kcl/mole while in the second stage it amounts to about 4kcl/mole. As a consequence, the reaction rate of atomic hydrogen is about eight orders of magnitude higher than the molecular hydrogen channel. Atomic hydrogen can also react with UF_5, reducing it to uranium tetrafluoride;

(UF_5) gas + H $\rightarrow$ (UF_4) gas + HF + 35.1 kcl/mole ..... (5)

Furthermore, two UF_5 molecules may undergo a disproportionation reaction, forming UF_4 and regenerating UF_6.

(UF_5) gas + (UF_5) gas $\rightarrow$ (UF_4) gas + UF_6 – 32.7 kcl/mole ..... (6)

Though the above reaction is endothermic, the condensation of gaseous UF_4 more than compensates for the consumption of heat:

(UF_4) gas $\rightarrow$ (UF_4) ss + 73.1 kcl/mole ..... (7)

Depending on the process conditions, in principle it is possible for the condensation of UF_5 molecules to be faster than the formation of UF_4. An analysis has shown that the final product of the reactions about an hour later after the cessation of the experiments is UF_4, which may be formed as a result of the disproportionation reaction; in this case the overall reaction assumes the form:

(UF_5) gas + (UF_5) gas $\rightarrow$ (UF_4)ss + 40.4 kcal/mole ..... (8)

Thus one may conclude that the overall reaction involving the reduction of UF_6 by hydrogen to the solid state is exothermic and is not limited by thermodynamic factors, although it does require an appreciable activation energy:

(UF_6) gas + H_2 $\rightarrow$ (UF_4)ss + 2HF + 71.8 kcl/mole ..... (9)

The UF_6/H_2 system provided an increase in quantum yield of the dissociation and in the yield of the target product (UF_5, UF_4). However judging from the above process chemistry, hydrogen may have adverse effect on the photolysis selectivity.

VIBRATIONAL PHOTOCHEMISTRY

UF_6 belonging to O_h point group has six normal modes of vibration. Out of these only the ν_3 and ν_4 modes give rise to rovibronic spectra proper, whereas the remaining modes are manifested in the spectrum by overtone vibrations. The reason for this is that the displacement of the center of gravity of charges occurs only in the ν_3 and ν_4 vibrations. Fig. 2 represents the six normal vibrations and the small signal absorption spectrum of 235 and 238-UF_6 at various temperatures. Infrared photochemistry of UF_6 can be studied using the more intense ν_3 mode at 16μm.

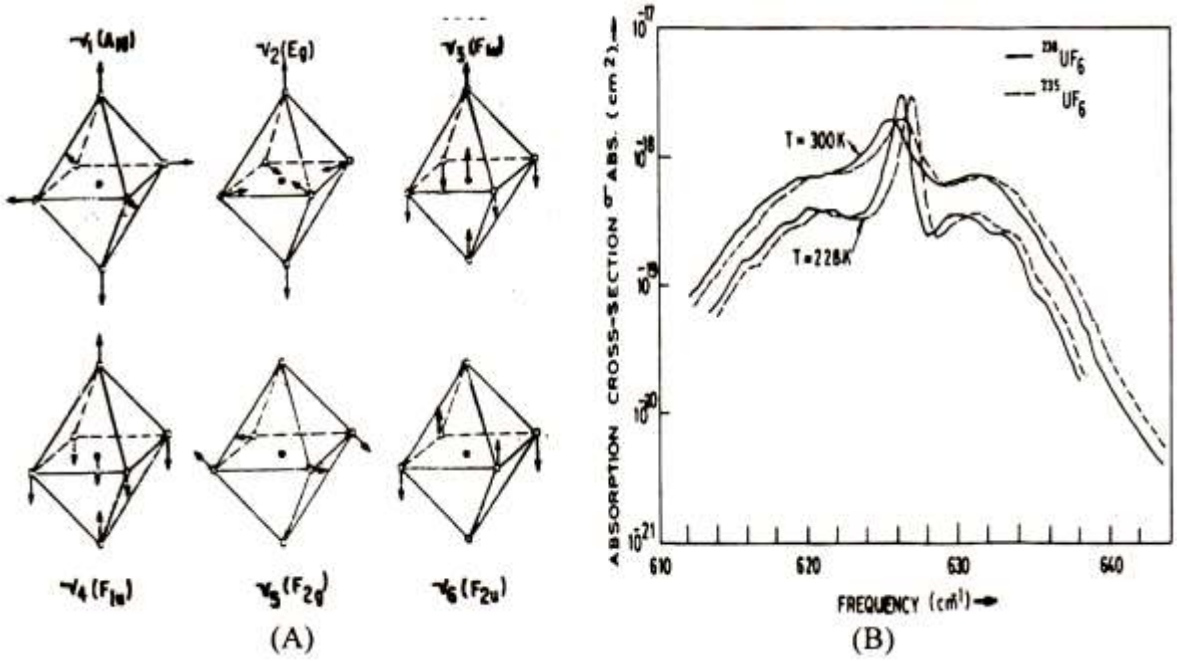

Fig. 2-(A) Six normal vibrations of UF_6 and (B) Small signal infrared absorption spectra of 235 & 238-UF_6 at two different temperatures.

We have carried out a theoretical estimate of multiple photon dissociation rate constants for UF_6 using 16μm laser. Using RRKM formalism, it has been shown that about 15 excess photons over the dissociation threshold (*Eo*=68 kcal mole^{-1}). i.c., about 50 laser photons are required for dissociation of each UF_6 molecule. Fig. 3 presents the unimolecular RRKM rate constant as a function of internal energy content of activated complex. Curve (a) is calculated with activated complex frequencies which are 0.95 times and curve (b) 0.65 times the corresponding frequencies of UF_6. The upper scale is in terms of excess photons of 16 μm laser above the dissociation threshold.

Further the laser fluence requirements for creating such massive multiphoton excitation can be evaluated using energy grained master rate equation (EGME). In general, it has been found that higher laser fluxes will populate higher and higher quantum states in polyatomic molecules within a limited energy spread. The fluence dependence of dissociation yield has been measured experimentally and it was found that MPD of UF_6 occurs with a threshold of 1 – 1.2 J cm^{-2}. Using the rate equation model, we have shown[4] that the dissociation yield can satisfactorily be evaluated and agreed well with the experimental data in the working pressure range of 1-2 Torr.

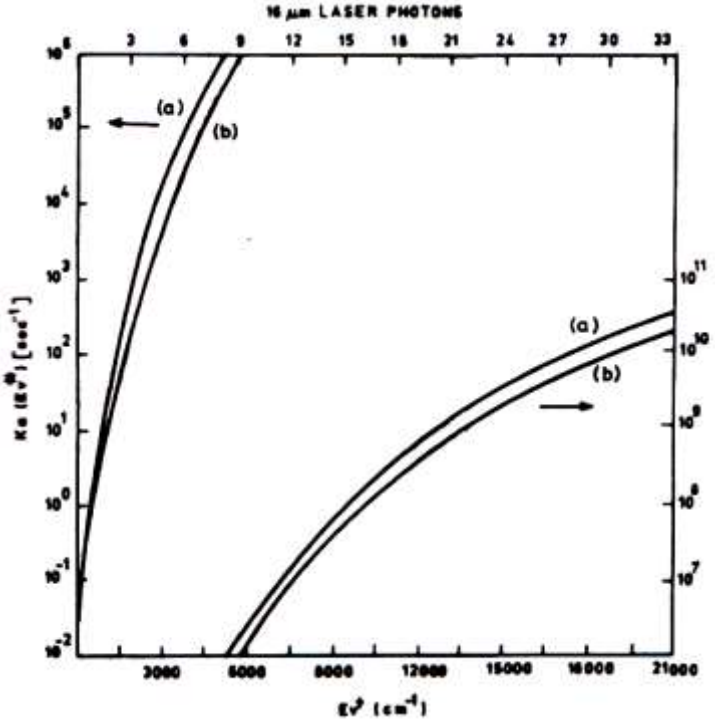

Fig. 3- Unimoleculter RRKM rate constant as a function of internal energy content of activated complex.

From the point of view of isotopic selectivity, two parameters, which are of interest, are -

1. What should be the optimum level of energization for UF_6 molecule to dissociate without collisional energy exchange and
2. What laser fluencies are required to achieve this energization.

The mean colloisional time for 235- UF_6 collisions at 1 Torr natural UF_6 is 285 ns. The random life time for an energized UF_6 molecule at 15 excess photons is about 10–20 ns. Within a typical laser pulse of 200 ns, we can therefore expect about 10% loss of 235-UF_6 excited at 13–15 excess photons i.e., about 50 laser photons.

It is well known that there is no measurable absorption of CO_2 laser (9-11 μm) radiation by UF_6 at room temperature, even through its hot bands. (Absorption cross section of 5.3 x 10^{-7} $torr^{-1}cm^{-1}$). However, IR photochemistry of UF_6 was conveniently studied9 using CO_2 laser under near resonant V-V energy transfer from various sensitizers like SF_6, CF_3Cl, CF_2Cl_2 etc. having good absorption in CO_2 laser region. The criteria for choosing such sensitizers, in particular the halomethanes are:

1. They have a varying absorption ranging from weak (combination band) to strong (fundamental) in the CO_2 laser region;
2. They have favourable vibrational levels for energy transfer processes;
3. Their dissociation energy is higher than UF_6 and
4. They are chemically inert towards UF_6.

A Lumonics 103-2 grating tuned TEA CO_2 laser having 100 ns initial spike followed by a 1 μs tail operation gat 0.5 Hz was used as the excitation source for the absorbers. The irradiations involving UF_6 were carried out in 10 cm. long and 100 cm^3 volume nickel cell equipped with monel valve and polished KCl end-windows on viton 0-rings. The relative changes in the sample concentrations were monitored by IR spectrometry (Perkin Elmer 577) at appropriate wavelengths for measuring the cell averaged dissociation yield per pulse.

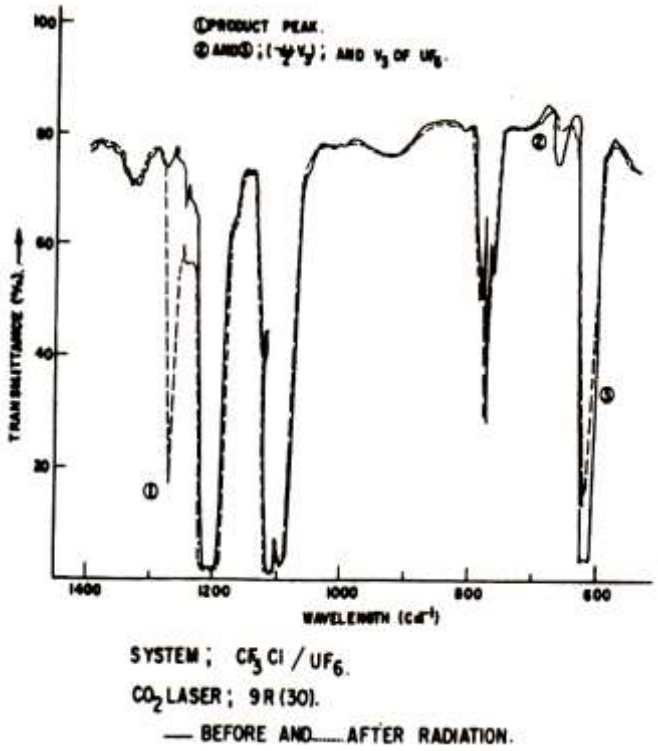

Fig. 4- IR spectra of CF_3Cl/UF_6 mixture before and after CO_2 laser irradiation

The roles of various experimental parameters like exciting frequency, fluence and pressure of sensitizer/acceptor on the dissociation processes were studied. Fig. 4 shows the IR spectrum of CF_3Cl/UF_6 mixture recorded before and after laser irradiation. One can clearly notice the decrease in UF_6-ν_3 absorption and appearance of new product peak. The efficiency of the energy transfer process was estimated on the basis of long range dipole–dipole interaction. This gave fruitful information about the dissociation mechanism relating the role of the absorption characteristics of the sensitizer and relative energy levels of the sensitizer and acceptor molecules. Overall processes occurring can be is summarized as follows talking CF_2Cl_2 as the sensitizer:

1. Multiphoton Absorption (MPA) by CF_2Cl_2:

$$CF_2Cl_2 \xrightarrow[9R(30)]{<n>h\nu} CF_2Cl_2^*\ (n\ \nu_2) \qquad \text{.....(10)}$$

2. Intermode Relaxatio: $CF_2Cl_2^*$

$$(n\ \nu_2) \xrightarrow{pt_{vv}} CF_2Cl_2^*(n\ \nu_m) \qquad \text{.....(11)}$$

3. V – V transfer : $CF_2Cl_2^*(n\ \nu_m) + UF_6$

$$\rightarrow UF_6^*(n\ \nu_3) + CF_2Cl_2 \qquad \text{.....(12)}$$

4. MPA by UF_6^*: $UF_6^*\ (n\ \nu_3)$

$$\xrightarrow{<m>h\nu} UF_6^{**} \rightarrow UF_5 + F \qquad \text{.....(13)}$$

In dealing with the mechanism of vibrational energy flow in polyatomic molecules whose specific vibrational mode is excited by a laser, it is the general consensus that the intramode V–V dominates the intermode V–V energy transfer. Therefore, a local vibrational quasi-equilibrium distribution is attained within the laser-pumped mode prior to the establishment of the steady state distribution among all the modes. In the final stage of relaxation the V–T/R energy transfer occurs from modes having low fundamental frequencies.

The role of V–V energy transfer being undoubted in the present studies, we can estimate the vibrational relaxation probabilities in each case on the basis of long range dipole-dipole interaction. The robability for transition from state 1 to state 2 induced by a time-dependent perturbation V (t) in the first order Born approximation is given by:

$$P_{12} = h^{-2} \left| \int_{-\infty}^{+\infty} V_{12}\ (t) \exp(i\Delta\omega t) dt \right|^2 \quad \text{.....} \quad (14)$$

Where $V_{12}(t) = < 1| V(t) | 2 >$ and $\Delta\omega$ is the frequency difference.

Evaluating the Born approximation, the vibrational relaxation probability for non-resonant ($\Delta\omega \neq 0$) transfer under the Sharma-Brau cut-off is given by:

$$< P> = (4\pi^4 C^2 \Delta\omega\mu/\sqrt{3} h^2 d^3 \nu^* kT) \exp(-\mu\nu^{*2} / 2kT) \quad \text{.....} \quad (15)$$

Where $C=1/3[d.m.^A]_{12}$ x $[d.m.^B]_{12}$ where $[d.\ m.^A]_{12}$ is the $1\rightarrow2$ vibrational dipole matrix element for molecule A and ν^* is given by $(2d\Delta\omega kT^{\mu-1})^{1/3}$. The above relation gives a behavior similar to that given by SSH theory i.e. in $< P > \approx \Delta\omega 2/3$ and $\approx T^{-1/3}$. These matrix elements can be determined from measurements of the integrated infrared absorption (S_m) which is related to them by:

$$d.\ m. = 0.3646\ (Sm/\nu)^{1/2} \quad \text{.....} \quad (16)$$

Where d.m. is in Debye, S_m in km mole^{-1} and ν is the band centre frequency in cm^{-1}.

From the available spectroscopic and kinetic data, the vibrational energy transfer probabilities were evaluated for UF_6/sensitizer systems using the above treatment. For one-quantum transfer, the probabilities are given in Table-1 which indicates that energy transfer can occur to UF_6 very efficiently from CF_2Cl_2 and SF_6. The estimated one-quantum transfer probability in the SF_6/UF_6 system agrees with the value of 2.8 x 10^{-11}cm^{3}s^{-1} at 300 K reported in the literature.

Once the vibrational energy transfer cross sections are known, the whole process can be described by a rate equation in a similar formalism to the energy grained master equation. The difference here is that the optical pumping terms are replaced by collisional pumping. Such excitation can either proceed to the dissociation threshold or it can result in the excitation of UF_6 in its quasi-continuum (QC) as discussed earlier. In the first case, the above rate equation can describe the whole process, while in the latter case further absorption of laser photons by QC-excited UF_6 molecules must include optical pumping terms at an appropriate time in the rate equation which requires a very careful analysis. The collisional pumping rates depend on the vibrational population of the sensitizer which is governed by the working laser fluence and molecular absorption cross section at the exciting frequency. Therefore, when the estimated energy transfer probabilities of the three sensitizers are normalized with respect to the absorption strength of ν_3 of SF_6, it is found that CF_3Cl is about fifty times less efficient than CF_2Cl_2 and that CF_4 is almost ineffective in inducing dissociation of UF_6 due to its poor absorption and strong radiative coupling of the pumped mode to ν_2 instead of the required ν_4 mode.

Table 1

[Vibrational energy transfer probabilities for various sensitizers with UF_6 (ν_3=625cm^{-1}; d.m.=0.38D) using long – range dipole-dipole interaction.]

Molecule	Pumpmode (cm^{-1})	Dipole moment	Laser line (cm^{-1})	Transfer mode (cm^{-1})	Dipole moment (D)	C(S/UF_6) (ergcm^3)x10^{40}	Probability <p>
CF_4	$\nu_2+\nu_4$ 1067	0.0099	9R(12) 1073	ν_4 630	0.053	67.64	0.0276
CF_3Cl	ν_t 1105	0.226	9R(30) 1084	ν_2 781	0.069	87.40	0.0062
CF_2Cl_2	ν_1 1101	0.183	9R(30) 1084	ν_2 667	0.198	250.80	0.369
SF_6	ν_3 948	0.388	10P(20) 944	ν_4 615	0.134	169.70	0.239
UF_6				ν_3 625	0.380		

The fact that parts of the energy absorbed get transferred to UF_6 was verified in a separate study by looking at the infrared fluorescence (IRF) of CF_2Cl_2 at 9.6 pm and of UF_6 at 16 μm in a laser excited CF_2Cl_2/UF_6 mixture. It was observed that simultaneously with the increase of <n> with UF_6 pressure, there is a decrease in 9.6 μm fluorescence and a growth of 16μm fluorescence intensity. The observed decrease of 9.6 μm intensity could be understood as the energy was siphoned off to UF_6 from CF_2Cl_2 via V-V energy transfer while the increase in 16 μm fluorescence is caused by IRF from such excited UF_6 molecules. The fast rise of 16 μm IRF (<1μs limited by the rise time of the detection system) suggested that intermolecular V–V energy transfer from CF_2Cl_2 to UF_6 is complete within the laser pulse duration.

URANIUM TETRAYDROBORATE, $U(BH_4)_4$

$U(BH_4)_4$ offers the possibility of using the $(5f)_2$ electrons of U^{4+} for electronic transitions and in the tetrahedral site symmetry both magnetic and forced electric dipole transitions are allowed for pure electronic origins. Well over 200 transitions between 5000 and 30,000cm^{-1} were reported. The gas phase absorption spectra at room temperature showed a strong UV absorption band around 250 nm. In spite of the available spectroscopic data there have been very few photochemical studies reported to-date. In a flash photolysis study of $U(BH_4)_4$, emission lines of U I, U II and a molecular species BH in the regions 411-478 and 478 -0598 nm has been reported. Afterwards, enrichment of boron isotopes in the product B_2D_6 has been observed by TEA CO_2 laser irradiation of $U(BD_4)_4$. The compound did not seem to decompose under CW irradiation with either CO_2 or Ar^+ lasers but decomposed on UV irradiation at 253.7 nm. This molecule has also been identified as a prospective candidate for LIS of uranium. The wavelength dependence of UV-promoted photochemistry has not yet been determined for this molecule. An interesting phenomenon like gas solid structural transitions exists in this compound and such structural dynamics, presumably involving facile U-H-B bridge bond rearrangements, is expected to generate an unusually interesting photochemical process. In the present investigation[10] we report the photochemical behavior of U $(BH_4)_4$ in different electronic origins using UV and visible radiation. The determination of the products at various photolyzing wavelengths provides an opportunity to look into the complex nature of the photodecomposition process.

U $(BH_4)_4$ was prepared by the method as described in the literature. It was purified by vacuum sublimation and kept in a sealed evacuated ampoule. The compound was characterized by its X-ray powder pattern and mass spectrometry. The vapour phase absorption spectrum in the UV region was taken using a 10 cm long cell, which showed a broad absorption feature with maxima near 250 nm. The peak absorption

cross section was estimated to be 8.9 x 10^{-18} cm^2. The solution phase spectra (4-5 mM) in solvents liked n-heptane and diethyl ether were recorded to obtain the weak absorption characteristics in the visible region.

The Pyrex photolysis cell was 100 cm long and 2.5 cm in diameter, fitted with quartz end-windows, and was provided with a cold finger into which the sample can be vacuum distilled using a liquid nitrogen trap. Typical photolysis were carried out at room temperature (0.08 Torr) and 48°C (1.2 Torr) for 2 h with a UV – vis radiation provided by a 450 W high pressure xenon lamp. The light beam was collimated with proper quartz optics and the photon flux was determined by uranyl oxalate actinometer. A UV cut-off Pyrex filter before the cell provided broad band visible radiation (> 300 nm). A homemade pulsed ruby laser was used for photolysis at 694.3 nm. The laser consisted of a 7.5 cm long and 6mm diameter ruby rod, which was optically pumped by two xenon flash lamps. The laser pulse energy was 0.7 J, with pulse duration of 700 μs. for irradiation at 632.8 nm, a 2 m W He-Ne laser was used for which no detectable decomposition was observed, even after a long exposure time. This could be due to very poor absorption of the sample at this wavelength and also low power of the laser used.

The total gaseous products were measured in the vacuum-line using a Toeppler pump and Saunders –Taylors apparatus, and the hydrogen content was estimated by combustion technique using hot (300°C) cupric oxide. The other product, namely diborane B_2H_6, was characterized and estimated by IR spectrometry. Mass spectrometric analyses were also carried on the total gas mixture for counterchecking the estimated products.

After photolysis, the non – volatile red brown solid deposit on the cell walls was dissolved in a concentrated HCl – H_2O_2 mixture. The solution was then analyzed for U-content by a fluorimetric technique by exiting at 360 nm and monitoring the resulting fluorescence at 550 nm. The boron content was determined by a colorimetric method by complexing with curcumin, which formed a red coloured rosacyanin complex.

A considerable decomposition was noticed in all experiments using UV (Hg lamp) and visible (uv-filtered Hg lamp and Ruby laser) radiation with B_2H_6 and H_2 as gaseous and $U(BH_4)_4$ as the solid products.

$$2U(BH_4)_4 \rightarrow H_2 + B_2H_6 + U(BH_4) \quad \text{.....(17)}$$

$$U(BH_4)_4 \rightarrow 8H_2 + UB_4 \text{ (or U + 4B)}$$

Fig. 5 shows the strong feature at 1601 cm^{-1} of B_2H_6 produced after photolysing for 2 h with a xenon lamp. Analysis of the U / B ratio of the solid deposit and its UV – vis absorption indicated it to be uranium trihydrborate $U(BH_4)_3$. Quantum yield for hydrogen at 253.7 nm was fond to be 0.25 and the quantum yield for hydrogen increased as the excitation wavelength becomes linger.

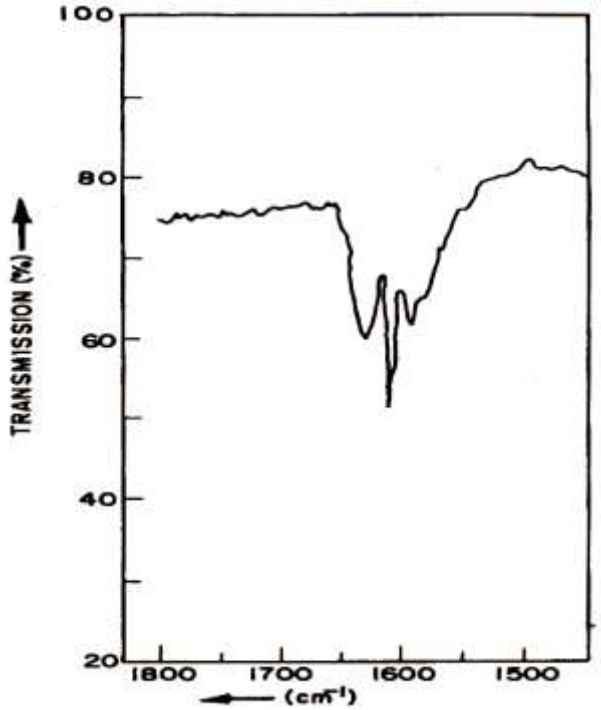

Fig. 5-IR spectrum of B_2H_6 produced in the photolysis of $U(BH_4)_4$

Although the stoichiometry and relative yields were generally reproducible, the absolute yields seemed to be dependent on the cell surface condition and solid deposit present, if may. However, The large net yield and high quantum yield of H_2 with 694.3 nm ruby laser photolysis suggest a "molecular collapse" of $U(BH_4)_4$. In the gas phase, the molecular symmetry is Td and each boron atom is attached to the central uranium atom by three hydrogen bridges [cf. Fig 6]. Since the hydrogen bonds are rather weak (few kcal / mole), the collapse occurs by knocking off the hydrogen bridges. Thus H atoms and BH radicals generated tend to give larger net yields of hydrogen. The differences observed in the product ratio for different photolysis wavelengths were probably due to different electronic transitions involved (Table 2).

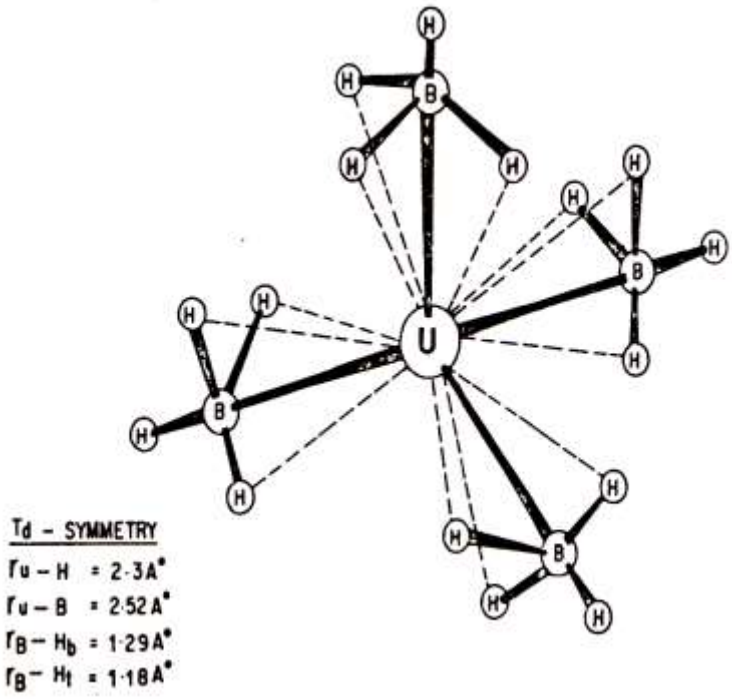

Fig. 6-Structure of the tetrahedral $U(BH_4)_4$ molecule showing the hydrogen bridges.

Uranyl hexafluoro-acetylacetonate tetrahydrofuran $UO_2(hfacac)_2$. THF

Since UF_6 does not absorb cheap laser photons from an efficient CO_2 laser, it is desirable to synthesize volatile and stable uranium compounds which can absorb CO_2 laser radiation. Therefore, we have synthesized a large (44 atoms) and complex compounds UO_2 (hfacac)$_2$. THF [cf. fig. 7] and studied its IRMPD by TEA CO_2 laser11. The compound has a rather low vapour pressure (about 10^{-3} Torr) at room temperature while at moderate temperatures; it is reasonably volatile (about 0.7 torr at 100°C). The O–U–O asymmetric stretch of the uranyl moiety is in resonance with a number of transitions of the 10.6 μm CO_2 laser radiation and is spectroscopically selective for the isotopes of both uranium and oxygen. The uranium isotope shift is about 0.7 cm^{-1} and as such IR absorption features are not spectrally resolved. However, with a suitable choice of the absorbing laser lines selected uranium isotopes can be preferentially excited and dissociated.

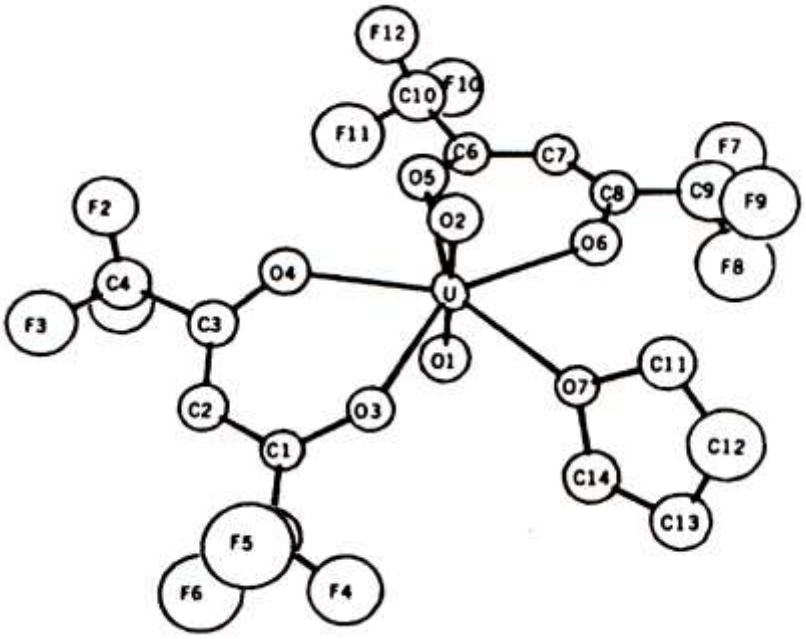

Fig. 7- Structure of large molecule UO_2 (hfacac)$_2$. THF containing 44 atoms

Table 2

[Probable assignment of electronic origins for various excitation wavelengths.]

Origin (Rel. intensity)	Exciting Wavelength (nm)	Typical quantum yield $\phi(H_2)$	Transition*	Vibrational assignment
Origin "n" at 13831cm^{-1}(100)	694.3	~8	$E(^3H_4) \rightarrow T_2(b\text{-}^3H_6)$	n + 572 cm^{-1} i.e., $n + \nu_n + \nu_\beta$
Origin "P" at 15400 cm^{-1}(11)	632.8	…	$E(^3H_4) \rightarrow E(^1D_2)$	P + 363 cm^{-1} i.e., $p + 2\nu_\delta$
Origin "e" at 24795 cm^{-1}(27)	UV cut-off visible (>300 nm)	0.59	$E(^3H_4) \rightarrow T_2(^3P_2)$	Ee + 1850 cm^{-1} i.e., $ee + \nu_\theta$

*on the basis of Zeeman effect data, the lack of EPR data and the density of transitions observed, the ground state of $U(BH_4)_4$ is taken as E ($^3H_4$)

For this purpose, we first undertook the small signal IR absorption studies, mass spectral characterization and thermal stability studies of this compound. Then we have performed selective photodissociation of isotopic molecules with overlapping IR absorption bands with a low-density molecular beam of the compound interacting with a line-tunable TEA CO_2 laser. Dissociation of the compound was

observed as a decrease in molecular beam intensity. The schematic of the experimental arrangement is shown in Fig. 8. The molecular beam source was operated between 25 and 95°C for all the measurements made. However, the measurements reported here were carried out at 85°C oven temperature. The laser beam intercepted the molecular beam 3 cm upstream of the ionizer entrance at right angle to the particle beam. The emerging laser beam was detected by a photon drag detector. The output of this detector triggered a signal average with 2048 channels and 5 μs dwell time per channel. The laser used was a grating-tuned Lumonics 103-2 TEA CO_2 laser. The temporal profile of the laser pulse, as monitored by photon drag detector, consisted of a 100 ns spike followed by a few μs tails. The laser beam was collimated to a spot of 1cm diameter. Different lines P(4), P(6), P(10) and P(20) of the 10.6 μm band of the CO_2 laser were used with the flounce level maintained at 85 mJ / cm^2 at repetition rate of 0.5 Hz.

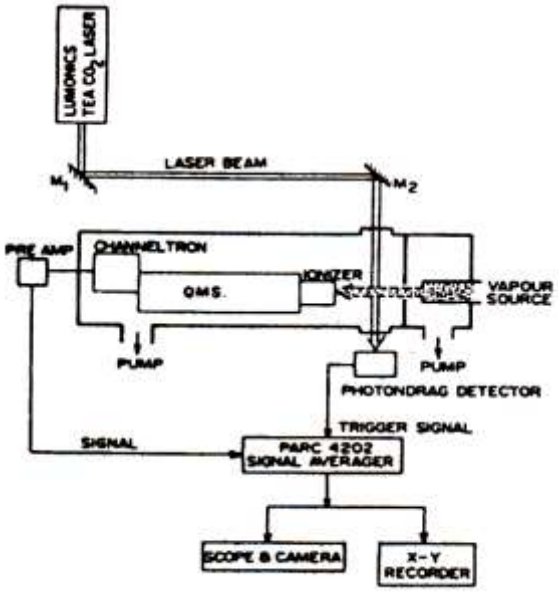

Fig. 8-Schematic of the molecular beam set up for isotope selective dissociation of $UO_2(hfacac)_2.THF$

The fractional depletion of 238-U and 235-U species in the parent compound as a result of laser photolysis was therefore measured by tuning the mass filter to *m/e* at 549(238-$UO_2[CF_3CO]_2THF^+$) or *m/e* at 546 (235-$UO_2[CF_3CO]_2CH.THF^+$) ion peaks and recording the laser-induced deletion in these ionic signals. The output of the signal average, averaged over several thousand laser shots (typically 3000 shots) were used to calculate fractional decomposition of the process:

$$<n> h\nu\ {}^{i}UO_2(hfacac)_2.THF \rightarrow {}^{i}UO_2(hfacac)_2. + THF(i=235\ o\ 238) \quad \text{.....……..} \quad (19)$$

Monitoring of the parent mass peaks produced identical results. No detectable decomposition was observed either by using off-resonant P(20) laser line or by setting the mass filter to the valley of 546(235-U species) and 549(238-U species) peaks corresponding to any other absorbing laser line. The latter study established the stability of the mass setting of the quadrupole mass filter over the entire experimental runs. The results obtained are presented in Table 3.

Table-3

[Isotope selective dissociation of $UO_2(hfacac)_2.THF$

Laser flounce: 85 mJ cm^{-2}, Temperature: 85°c Feed material used natural uranium with 0.72% U-235]

Laser line(cm^{-1})	U-isotope	Dissociation (%)	Isotopic composition (%) U-bearing product	Isotopic composition (%) Undecomposed feed	Remarks
10P(4)	235	16.0	0.81	0.71	235-U selective
957.81	238	14.3	99.19	99.29	
10P(6)	235	8.8	0.21	0.94	238-U selective
956.20	238	30.0	99.79	99.06	
10P(10)	235	--	--	--	Exact Decomposition in235-U could not be measured; However, selectivity of 238-U in product indicated
952.89	238	11.0	--	--	
10P(20)	235	--	--	--	10P(20) line being off-resonant is not absorbed by the sample
944.21	238	--	--	--	

For P(6) laser line, the decomposition was found to be linear as a function of laser fluence in the range of 30 to 155 mJ / cm^2. The mulltiphoton absorption and dissociation properties of the molecule indicted a very low vibrational quasi-continuum limit with state density of about 10 per cm^{-1} at energy of 105000 cm^{-1}. Excitation of the 0→1 vibrational transition quickly relaxes transferring excitation to a few tightly coupled modes and the pumped mode return to its ground state where it can continue to absorb many more laser photons. Incidentally tuning the laser line appropriate to desired isotopic component we have also demonstrated isotopic separation of uranium. Although the selectivity factors in beam experiments are promising, studies in static or flow cell configuration showed much greater complexity and negligible isotopic selectivity in dissociation.

REFERENCES

[1] Paine, R. T., Schonberg, P. R., Lihgt, R. W.,Danen, W. C. & Freund, S. M. (1979) *J. Inorg. Nucl. Chem*. 41 : 1577

[2] Subbiah, J., Sarkar, S. K., Rama, Rao, K. V. S., & Mittal, J. P. (1980) *Ind. J. Phys*. 54B : 121

[3] Talukdar, R. K., Bajaj, P. N., Sarkar, S. K., Chakraborty, P. K. (1981) *Proc. IInd National Symp. On Mass Spectrometry*, BARC, Bombay.

[4] F. S. Becker, K. L. Kompa. (1982) *Nuclear Technology*, *58* (2), 329-353.

[5] Kim, K. C., Freund, S., Sauuder, R.K., Smith, D. F. & Person, W. B. (1983) *J. Chem. Phys.* 78 : 32

[6] Sarkar, S. K. & Karve, R. S. (1984) in *lasers and Applications*, (ed.) Bist, H. D. & Goela, J. S., New Delhi, McGraw-Hill, p. 401

[7] Lyman, J. L. & Holland, R (1987) *J. Phys. Chem*. 9 : 4821

[8] Karve, R. S., Sarkar, S. K., Rama Rao, K. V. S. & Mittal, J. P. (1991) Appl. Phys B53 : 108

[9] Sarkar, S. K., Rama, Rao, K. V.S. & Mittal, J. P. (1992) *Polyhedron* 21 : 2783

[10] D.L. Schulz, D.S. Richeson, G. Malandrino, D. Neumayer, T.J. Marks, D.C. DeGroot, J.L. Schindler, T. Hogan, C.R. Kannewurf. (1992) *Thin Solid Films* **,** *216* (1) , 45-48.

[11] Wolfgang A. Herrmann, Norbert W. Huber, Oliver Runte. , (1995) *Angewandte Chemie* **,** *107* (20) , 2371-2390.

[12] Larry R. Avens,, David M. Barnhart,, Carol J. Burns, and, Steven D. McKee. (1996) *Inorganic Chemistry***,** *35* (2), 537-539.

[13] Marianne P. Wilkerson,, Carol J. Burns,, Harry J. Dewey,, Jerod M. Martin,, David E. Morris,, Robert T. Paine, and, Brian L. Scott. (2000) *Inorganic Chemistry*, *39* (23), 5277-5285.

[14] Gulaim A. Seisenbaeva,, Lars Kloo,, Pia Werndrup, and, Vadim G. Kessler. (2001) *Inorganic Chemistry*, *40* (15), 3815-3818.

[15] D.C. Bradley, R.C. Mehrotra, I.P. Rothwell, A. Singh. (2001)X-Ray Crystal Structures of Alkoxo Metal Compounds, 229-382.

[16] C.J. Burns, M.P. Neu, H. Boukhalfa, K.E. Gutowski, N.J. Bridges, R.D. Rogers. (2003) The Actinides. **,** 189-345.

[17] Robert D. Mcalpine, D. K. Evans. (2007) Laser Isotope Separation by the Selective Multiphoton Decomposition Process. 31-98.

[18] Robert D. Mcalpine, D. K. Evans. (2007) Laser Isotope Separation by the Selective Multiphoton Decomposition Process, 31-98.

[19] Skye Fortier, Guang Wu, Trevor W. Hayton. (2008) *Inorganic Chemistry*, *47* (11), 4752-4761.

[20] Linus Appel, Jennifer Leduc, Christopher L. Webster, Joseph W. Ziller, William J. Evans, Sanjay Mathur. (2015) *Angewandte Chemie* **,** *127* (7) , 2237-2241.

[21] Falcone, M., Chatelain, L., Scopelliti, R., Zivkovic, I. & Mazzanti, M. (2017) *Nature* **547**, 332–335.

[22] Barluzzi, L., Chatelain, L., Fadaei-Tirani, F., Zivkovic, I. & Mazzanti, M. Facile. (2019)*Chem. Sci.* **10**, 3543–3555.

[23] Alcone, M. et al. (2019) *Nat. Chem.* **11**, 154–160.

[24] Grigorii N. Makarov. (2022) *Uspekhi Fizicheskih Nauk* **,** *192* (06) , 569-608.